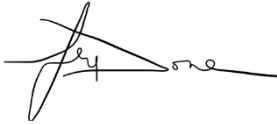




Technical Note on Quality Assessment for Jilin-1 GP01/02

Author(s): 
_____ **Sam Lavender**
Task 1 Mission Expert

Approval: 
_____ **Fay Done**
Task 1 Lead

Accepted: 
_____ **Clement Albinet**
EDAP Technical Officer

TABLE OF CONTENTS

1. EXECUTIVE SUMMARY	4
2. INTRODUCTION.....	6
2.1 Reference Documents	6
2.2 Glossary	7
3. EDAP QUALITY ASSESSMENT	9
3.1 EDAP Maturity Matrix.....	9
3.2 Summary Calibration / Validation Maturity Matrix	11
3.2.1.1 Product Information	11
3.2.1.2 Metrology	12
3.2.1.3 Product Generation.....	13
3.2.2 Validation Calibration / Validation Maturity Matrix Assessment	14
4. DETAILED JILIN-1 GP01/02 QUALITY ASSESSMENTS.....	16
4.1 Objectives	16
4.2 Product Image Quality.....	16
4.2.1 Visual Inspections.....	16
4.2.1.1 Method	16
4.2.1.2 Results	16
4.2.2 Signal-to-Noise Ratio.....	17
4.2.2.1 Method	17
4.2.2.2 Results	18
4.2.3 Modulation Transfer Function.....	21
4.2.3.1 Method	21
4.2.3.2 Results	21
4.3 Geometric Calibration Quality	21
4.3.1 Absolute Geolocation Accuracy.....	21
4.3.1.1 Method	22
4.3.1.2 Results	22
4.3.2 Temporal Geolocation Accuracy	24
4.3.2.1 Method	24
4.3.2.2 Results	25
4.3.3 Band Co-registration Accuracy.....	26
4.3.3.1 Method	26
4.3.3.2 Results	26
4.4 Radiometric Calibration Quality.....	27
4.4.1 Absolute Radiometric Calibration Accuracy	27
4.4.1.1 Method	27
4.4.1.1.1 Comparison to RadCalNet.....	27
4.4.1.1.2 Comparison to CHRIS/Proba-1	30
4.4.1.2 Results	31
4.4.1.2.1 Comparison to RadCalNet.....	31
4.4.1.2.2 Comparison to CHRIS/Proba-1	33
4.4.2 Temporal Radiometric Accuracy	34
4.4.2.1 Method	34
4.4.2.2 Results	34
5. CONCLUSIONS.....	35
APPENDIX A HYPERSCAN TEST DATASET	36

AMENDMENT RECORD SHEET

The Amendment Record Sheet below records the history and issue status of this document.

ISSUE	DATE	REASON
0.1	18 10 2021	First draft for ESA review
1.0	13 04 2022	Final version after feedback addressed

1. EXECUTIVE SUMMARY

HyperScan is carried onboard the Jilin-1 GP01 and Jilin-1 GP02 Earth Observation (EO) satellites, which were both launched on 21 January 2019 from the Jiuquan Satellite Launch Centre in China. The missions are operated by Chang Guang Satellite Technology Co. Ltd, a commercial spinoff of the Chinese Academy of Sciences, with HEAD Aerospace Group acting as the data provider for EDAP.

It is important to note that whilst HyperScan is commonly referred to a hyperspectral mission in the mission literature, it is a mission which collects data for a high number of bands from a combination of Visible Near-Infrared (VNIR), Shortwave, Mediumwave and Longwave Infrared imagers rather than a high number of bands from one imager (i.e. hyperspectral).

Table 1-1: Mission - Jilin-1 GP01/02: Assessment Area Results

Assessment Area	Results
Visual Inspections	The visual inspections, performed on the nineteen VNIR bands of all acquisitions (with the panchromatic band being the first VNIR band), did not show any gross anomalies or artefacts. See Section 4.2.1.
Image Quality	<p>Signal-to-Noise Ratio: The results of the Signal-to-Noise Ratio (SNR) assessment, performed on the acquisitions of Libya-4, indicate higher SNR values than those supplied in their product quality files. The methodology applied by the data provider is not known. So, the different values could result from different approaches / targets with different brightness' as the reference radiance is a key determinant of the SNR. However, the conclusion is that what is provided is probably an underestimate and so does not overstate what is possible. See Section 4.2.2.</p> <p>Modulation Transfer Function: A Modulation Transfer Function (MTF) assessment was not possible as the spatial resolution of the VNIR sensor is too large for the MTF target in Salon-de-Provence (France). See Section 4.2.3.</p>
Geometric Calibration	<p>Absolute Geolocation Accuracy: The results of the geometric calibration quality assessment indicate general agreement with the geolocation accuracy performance requirement, detailed in the HyperScan datasheet [RD-3], of < 20 m (unknown if RMSE or CE90 as not specified by provider). For two acquisitions, the northing error was greater than 20 m, but the assessment was performed for a relatively small number of both GCPs and acquisitions. See Section 4.3.1.</p> <p>Temporal Geolocation Accuracy: The temporal geolocation accuracy assessment results indicate that the northing direction (along-track (y)) accuracy may be less accurate than easting direction (across-track (x))</p>

	<p>and can be larger than the pixel size. Therefore, applying additional georeferencing using GCPs (not used) could improve the georeferencing accuracy. However, this result is based on assessing two products from two different sites, so it has limited applicability. See Section 4.3.2.</p> <p>Band Co-registration Accuracy: The results of the band co-registration accuracy assessment indicate that the accuracy is sub-pixel. However, this result is based on the evaluation of two products, so it has limited applicability. See Section 4.3.3.</p>
<p>Radiometric Calibration</p>	<p>Absolute Radiometric Accuracy: The result of the absolute radiometric accuracy assessment indicates the accuracy is low, when assessed using the top of atmosphere reflectance data from RadCalNet. This result is supported by comparisons to top of atmosphere reflectance data from Sentinel-2 and CHRIS/PROBA-1. See Section 4.4.1.</p> <p>Analysing a more significant number of acquisitions over a broader range of RadCalNet sites would confirm these findings that are currently for a limited number of acquisitions and sites. The supplied documentation [RD-4] does not indicate post-launch vicarious calibration has occurred, but a separate document [RD-5] was supplied providing some details on this. The Jilin-1 instruments are vicariously calibrated using MODIS surface reflectance data propagated to the top of the atmosphere, and modified calibration coefficients are used where the relative difference is greater than 10% [RD-5]. It is not clear from the metadata the source of the calibration coefficients used for the supplied products and whether this vicarious calibration has been applied.</p> <p>Temporal Radiometric Accuracy: The temporal radiometric accuracy assessment results are limited because of the limited number of acquisitions available, so it was difficult to draw definitive conclusions. See Section 4.4.2.</p>

2. INTRODUCTION

This technical note details the results of the preliminary data quality assessments (geometric calibration, radiometric calibration and image quality) performed on a sample of orthorectified bundle products generated for the Earth Observation (EO) satellite Jilin-1 GP01/02 (“HyperScan”).

The aforementioned data quality assessments are performed in accordance with the assessment guidelines, detailed in [RD-1, RD-2], that constitute the European Space Agency (ESA) Earthnet Data Assessment Pilot (EDAP) Project’s *EO Mission Data Quality Assessment Framework*. An important representation of the latter framework, constructed by the National Physical Laboratory (NPL, U.K), is what is known as the *maturity matrix*. It is a diagrammatic summary of the following:

- **Documentation Review:** *the EDAP Optical team reviews materials (e.g. ancillary / auxiliary data and documentation) provided by the mission provider (data provider and / or operator), some of which may not be publicly available, or even the scientific community (e.g. published papers). The results are detailed in Section 3 (covering the first section of the maturity matrix, see Table 3-1).*
- **Data Quality Assessments:** *the EDAP Optical team performs data quality assessments (i.e. validation assessments), independently of those performed by the mission provider. The results are detailed in Section 4 (covering the second section of the maturity matrix, see Table 3-2).*

The above data quality assessments are performed by the project’s Optical team using the appropriate in-house and open-source ad-hoc scripts / tools.

It is important to note the purpose of the *EDAP EO Mission Data Quality Assessment Framework* is to ensure the delivered commercial mission data (products) is fit for purpose and that all decisions regarding the inclusion of the commercial mission as an ESA third party mission can be made fairly and with confidence.

2.1 Reference Documents

The following is a list of reference documents with a direct bearing on the content of this proposal. Where referenced in the text, these are identified as [RD-n], where 'n' is the number in the list below:

- RD-1. EDAP Best Practice Guidelines, EDAP.REP.001, v1.2, September 2019.
- RD-2. Earth Observation Mission Quality Assessment Framework – Optical Guidelines, EDAP.REP.002, v2.0, December 2020.
- RD-3. Head Aerospace – HyperScan (JL-1GP-01/02) Data Sheet, v1.0 (2020)
- RD-4. Head Aerospace - Jilin-1 Imagery Product Guide, V1.1 (2021)
- RD-5. Head Aerospace - Radiometric Calibration of Jilin-1
- RD-6. <https://sentinel.esa.int/web/sentinel/user-guides/sentinel-2-msi/definitions>

- RD-7. Gascon, F., et al. (2017). Copernicus Sentinel-2A calibration and products validation status. *Remote Sensing*, 9, 584. <https://doi.org/10.3390/rs9060584>
- RD-8. Bouvet, M.; Thome, K.; Berthelot, B.; Bialek, A.; Czaplá-Myers, J.; Fox, N.P.; Goryl, P.; Henry, P.; Ma, L.; Marcq, S.; Meygret, A.; Wenny, B.N.; Woolliams, E.R. 2019. RadCalNet: A Radiometric Calibration Network for Earth Observing Imagers Operating in the Visible to Shortwave Infrared Spectral Range. *Remote Sens.*, <https://doi.org/10.3390/rs11202401>
- RD-9. Technical Note on Quality Assessment for DOVE-R, v1.0, EDAP.REP.016
- RD-10. Roy, D.P.; Li, J.; Zhang, H.K.; Yan, L.; Huang, H. 2017. Examination of Sentinel-2A multispectral instrument (MSI) reflectance anisotropy and the suitability of a general method to normalise MSI reflectance to nadir BRDF adjusted reflectance. *Remote Sens. Environ.*, 199, 25–38.
- RD-11. Lavender, S. et al. 2021. CHRIS/PROBA-1 Radiometric Calibration Assessment, 2021 11th Workshop on Hyperspectral Imaging and Signal Processing: Evolution in Remote Sensing (WHISPERS), 2021, pp. 1-5, <https://doi.org/10.1109/WHISPERS52202.2021.9483995>

2.2 Glossary

The following acronyms and abbreviations have been used in this Report.

BRDF	Bidirectional Reflectance Distribution Function
CEOS	Committee on Earth Observation Satellites
DEM	digital elevation model
EDAP	Earthnet Data Assessment Pilot
EO	Earth Observation
ESA	European Space Agency
GSD	Ground Sampling Distance
IFOV	Instantaneous Field of View
MTF	Modulation Transfer Function
NBAR	Nadir BRDF-Adjusted Reflectance
NIR	Near-InfraRed
NPL	National Physical Laboratory
SNR	Signal-to-Noise Ratio
SRTM	Shuttle Radar Topography Mission
TOA	Top of Atmosphere



VNIR

Visible Near-Infrared

3. EDAP QUALITY ASSESSMENT

3.1 EDAP Maturity Matrix

Table 3-1 Summary Calibration / Validation Maturity Matrix for HyperScan.

Data Provider Documentation Review			Validation Summary	Key
Product Information	Metrology	Product Generation		Not Assessed
Product Details	Sensor Calibration & Characterisation Pre-Flight 	Radiometric Processing 	Measurement Validation Method	Not Assessable
Availability & Accessibility	Sensor Calibration & Characterisation Post-Launch 	Geometric Processing 	Measurement Validation Results Compliance	Basic
Product Format, Flags & Metadata 	Metrological Traceability Documentation	Mission-Specific Processing 	Geometric Validation Method	Good
User Documentation 	Uncertainty Characterisation 		Geometric Validation Results Compliance	Excellent
	Ancillary Data 			Ideal

Table 3-2 The Validation Calibration / Validation Maturity Matrix for HyperScan.

EDAP Product Assessment					
Validation Summary	Detailed Validation				
Radiometric Validation Method	→	Absolute Calibration Method	Signal to Noise Method	Temporal Stability Method	
Radiometric Validation Results Compliance	→	Absolute Calibration Results Compliance	Signal to Noise Results Compliance	Temporal Stability Results Compliance	
Geometric Validation Method	→	Sensor Spatial Response Method	Absolute Positional Accuracy Method	Band-to-Band Registration Method	Temporal Stability Method
Geometric Validation Results Compliance	→	Sensor Spatial Response Results Compliance	Absolute Positional Accuracy Results Compliance	Band-to-Band Registration Results Compliance	Temporal Stability Results Compliance

3.2 Summary Calibration / Validation Maturity Matrix

3.2.1.1 Product Information

Product Details	
Product Name	<i>JL-1GP01/02 Bundle Standard Orthorectified</i>
Sensor Name	<i>HyperScan</i>
Sensor Type	<i>Optical – Hyperspectral including panchromatic, visible and shortwave infrared bands</i>
Mission Type	<i>Twin Satellites - JL-1GP01 and JL-1GP02</i>
Mission Orbit	<i>Sun-synchronous (528 km altitude)</i>
Product Version Number	<i>Unknown</i>
Product ID	<i>JL1GP[01,02]_PMS[1,2]_L3A</i>
Product Processing Level	<i>Level 3A (Standard Orthorectified) Geometrically and Radiometrically (Top of Atmosphere) Calibrated</i>
Measured Quantity Name	<i>Digital Numbers (DN) / Top of Atmosphere Radiance</i>
Measured Quantity Units	<i>DN converted to $W.sr^{-1}.m^{-2}.\mu m^{-1}$</i>
Stated Measurement Quality	<i>GEO Location is quoted as 20 m All supplied products are classed as Product Quality “A”. The breakdown of the latter is given in the product quality metadata file (containing additional quality evaluation information, not detailed in the user guide)</i>
Spatial Resolution (GSD @ nadir)	<i>Multispectral imager: 5 m (B0-B6) / 10 m (B7-B12) / 20 m (B13-B19) Shortwave infrared camera: 100 m Mediumwave infrared camera: 100 m Longwave infrared camera: 150 m</i>
Spatial Coverage	<i>Global</i>
Temporal Resolution	<i>Revisit time of 2 days (latitude dependence not stated)</i>
Temporal Coverage	<i>Mission Lifetime > 5 years</i>
Point of Contact	<i>contact@head-aerospace.fr</i>
Product locator (DOI/URL)	<i>The sensor products were made available upon request and provided via specific links</i>
Conditions for access and use	<i>Conditions for access and use has not been explicitly stated by the mission provider but it is assumed they are those typically associated with the restricted access and use of commercial data apply (for more information, contact sales team at contact@head-aerospace.fr).</i>
Limitations on public access	<i>Commercial purchase</i>
Product Abstract	<i>Not provided</i>

Availability & Accessibility	
<i>Grade: Not Assessable</i> <i>Justification: Relevant information not made available.</i>	
Compliant with FAIR principles	<i>The product information (included in product metadata, etc.) provided meets some of the FAIR principles only.</i>
Data Management Plan	<i>None.</i>
Availability Status	<i>The products for this sensor are made available upon request only.</i>

Product Format, Metadata & Flags	
<i>Grade: Good</i> <i>Justification: Data in a documented standard file format, with a reasonable set of documented metadata and data flags.</i>	
Product File Format	<i>Each band is stored as a GeoTIFF with the DN to radiance conversion in an XML metadata file alongside information on the geometry.</i> <i>The product naming convention(s) and format(s) is defined in the product guide [RD-4]. It is important for users to be aware that imagery time is Beijing local time rather than UTC.</i>
Metadata Conventions	<i>The convention is described in the Product Guide [RD-4], but no conformance to a convention is stated.</i>
Analysis Ready Data?	<i>No</i>

User Documentation		
<i>Grade: Good</i> <i>Justification: Some PUG and ATBD-type information available.</i>		
<i>Document</i>	<i>Reference</i>	<i>QA4ECV Compliant</i>
Product Guide	<i>Jilin-1 Imagery Product Guide V1.1 (2021)</i>	<i>No</i>
Sensor Data Sheet	<i>Jilin-1 HyperScan (JL-1GP-01/02) Data Sheet v1.0 (2020)</i>	<i>No</i>

3.2.1.2 Metrology

Sensor Calibration and Characterisation – Pre-Flight	
<i>Grade: Good</i> <i>Justification: Pre-flight calibration & characterisation covers most important aspects of instrument behaviour at a level of quality to be judged fit for purpose; spatial characterisation is missing.</i>	
Summary	<i>Before launch, a laboratory radiometric calibration experiment determined the spectral calibration, relative radiometric calibration and absolute radiometric calibration. The resulting spectral-response functions were supplied for use with the EDAP radiometric calibration assessment.</i>

References	<i>Jilin-1 Imagery Product Guide V1.1 (2021) Radiometric Calibration of Jilin-1 Satellites (Version and Date unknown)</i>
-------------------	---

Sensor Calibration and Characterisation – Post-Launch	
<i>Grade: Basic Justification: Post-launch calibration & characterisation is not entirely of a level of quality to be judged fit for purpose.</i>	
Summary	<i>Information is provided in the product guide on a list of corrections applied. EDAP was provided with a separate document providing further details for post-launch, but there is not clarity on how this will be accessible to users.</i>
References	<i>Jilin-1 Imagery Product Guide V1.1, 2021 Radiometric Calibration of Jilin-1 Satellites (version and date unknown)</i>

Metrological Traceability Documentation	
<i>Grade: Not Assessable Justification: Relevant information not made available.</i>	
Document Reference	<i>N/A</i>
Traceability Chain / Uncertainty Tree Diagram Available	<i>No information provided</i>

Uncertainty Characterisation	
<i>Grade: Good Justification: Use of the Guide to the Expression of Uncertainty in Measurement (GUM) approach and sources of uncertainty included.</i>	
Description	<i>Short description of pre-launch on-ground radiometric calibration, including evaluation of uncertainty.</i>
Reference	<i>Radiometric Calibration of Jilin-1 Satellites (Version and Date unknown)</i>

Ancillary Data	
<i>Grade: Basic Justification: Ancillary data somewhat documented.</i>	
Description	<i>Orthorectification using the SRTM90 DEM</i>
Reference	<ul style="list-style-type: none"> • <i>Product Metadata</i> • <i>Jilin-1 Imagery Product Guide V1.1, 2021</i>

3.2.1.3 Product Generation

Radiometric Processing	
<i>Grade: Basic Justification: Limited information provided on approach.</i>	

Description	<i>Limited details provided in the product metadata and accompanying documentation on the radiometric processing, including the cross-calibration with MODIS. It is not clear which, if any, of the provided scenes had the cross-calibration coefficients rather than ground calibration coefficients applied.</i>
Reference	<i>Jilin-1 Imagery Product Guide V1.1, 2021 Radiometric Calibration of Jilin-1 Satellites (Version and Date unknown)</i>

Geometric Processing	
<i>Grade: Basic Justification: Limited information provided on approach.</i>	
Description	<i>Limited details provided - some information in the metadata file e.g., that a DEM is used, the number of GCPs (zero for all products provided), and an overview of the approach in the product guide.</i>
Reference	<i>Jilin-1 Imagery Product Guide V1.1, 2021</i>

Additional / Mission Specific Processing	
<i>Grade: Basic Justification: Limited information provided on approach.</i>	
Summary	<i>Limited details provided in the metadata file and accompanying explanation in the Product Guide</i>
Reference	<i>Jilin-1 Imagery Product Guide V1.1, 2021</i>

3.2.2 Validation Calibration / Validation Maturity Matrix Assessment

This section is detailing the grading of the maturity matrix in Table 3-2.

Radiometric Validation Method	
<i>Grade: Good Justification: Methodology covers a fuller range of satellite measurements, using representative reference measurements. Uncertainty information is available for the RadCalNet data, but not used.</i>	
Description	<i>The radiometric validation method involves a comparison to RadCalNet data at La Crau alongside the extraction of the SNR over Libya-4. There was only one product for La Crau and Libya-4 and two for Barrax and Rame Head, so the temporal radiometric analysis is limited.</i>
Reference	<i>Detailed assessment is in Section 4.4</i>

Radiometric Validation Results Compliance	
<i>Grade: Not Assessable Justification: No specific information provided on the radiometric accuracy by the data producer/provider.</i>	

Description	<i>Operator assessment not provided.</i>
Reference	-

Geometric Validation Method	
<i>Grade: Basic</i>	
<i>Justification: The methodology used here covers a fuller range of satellite measurements, using representative reference measurements. Uncertainty information not available for reference data.</i>	
Description	<i>The absolute positioning accuracy is based on identified features. It was not possible to use the available GCPs based on GPS measured locations due to the spatial resolution of the data, which did not show the identified features. Band-to-band registration and temporal analysis are based on these identified features.</i>
Reference	<i>Detailed assessment is in Section 4.2.3</i>

Geometric Validation Results Compliance	
<i>Grade: Good</i>	
<i>Justification: Graded as good as the 20 m quoted is a reasonable number for the users but should ideally be more clearly specified in terms of how this number was generated.</i>	
Description	<i>The overall geolocation accuracy is quoted as 20 m in the HyperScan datasheet, and 50 m (CE90) in terms of the uncontrolled positioning accuracy by the operator (charmingglobe website). From the analysis conducted this is a reasonable number although it would be useful for users to understand how this was assessed, e.g. if this is calculated as the Circular Error and how it may vary on a band/imager basis.</i>
Reference	<i>HyperScan datasheet</i> http://www.charmingglobe.com/EWeb/product_view.aspx?id=676

4. DETAILED JILIN-1 GP01/02 QUALITY ASSESSMENTS

4.1 Objectives

This work aims to assess all core aspects of sensor data quality (geometric calibration, radiometric calibration, image quality) against performance requirements or specifications, using the sample of sensor products procured from the data provider.

4.2 Product Image Quality

This section describes the assessment of product image quality of the supplied sensor products in terms of the **Signal-to-Noise Ratio (SNR)** and **Modulation Transfer Function (MTF)**. Prior to performing the latter assessments, general **Visual Inspections** are performed.

4.2.1 Visual Inspections

General visual inspections were performed on the panchromatic and VNIR imagery included in the sample of products procured to ensure there were no gross anomalies or artefacts present.

4.2.1.1 Method

The approach was to load the data into the ESA SNAP tool and then visually inspect the data.

4.2.1.2 Results

HyperScan has VNIR bands of different spatial resolutions: B0~B6 (nadir):5 m; B7~B12 (nadir):10 m; B13~B19 (nadir):20 m B3~B5 (nadir):3 m [RD-4].

The HyperScan bands are stored as separate GeoTIFFs, and the different spatial resolution groupings have different georeferencing information with the number of pixels in the 10 m band files not being exactly twice the number of pixels in the 5 m band files for the x and y directions. For example, for product 1 (La Crau), B1 has 15 336 by 15 141 pixels while B7 has 7676 by 7534 pixels. Therefore, to account for this, the individual GeoTIFFs were merged using GDAL with the coarser spatial resolution bands resampled to band 0 (the panchromatic band).

The data procured included acquisitions over La Crau (France), Barrax (Spain), Rame Head (UK) and Libya-4 (Libya); see Figure 4-1. The images are created from the GDAL merged files.

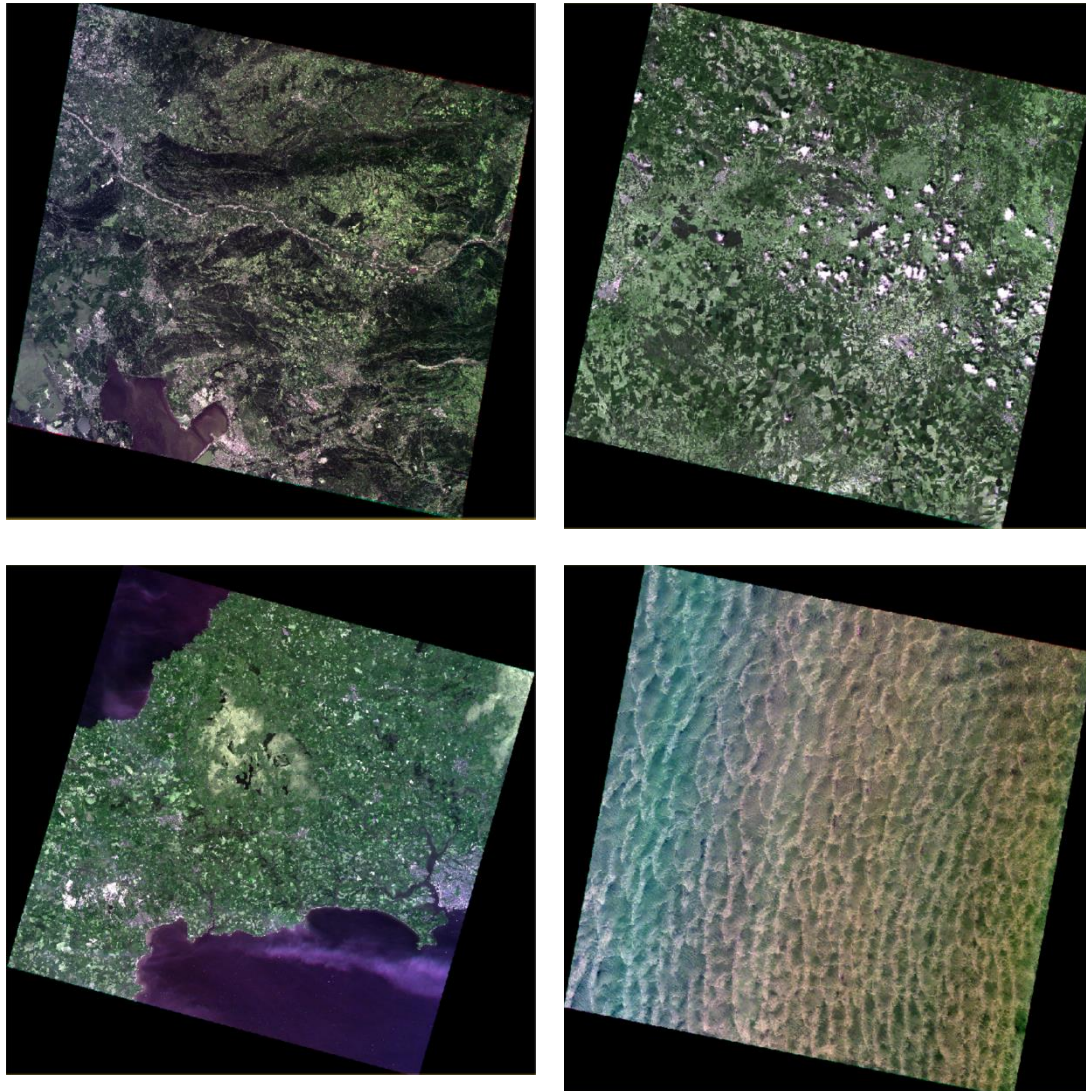


Figure 4-1: Examples shown are for La Crau, Barrax, Rame Head and Libya-4 (left to right and top to bottom) as the pseudo-true colour 5 m resolution data (bands for 655 [8], 562.5 [5] and 482.5 [3] nm).

4.2.2 Signal-to-Noise Ratio

4.2.2.1 Method

The SNR is used to quantify the performance of a sensor in response to a particular exposure; it quantifies the ratio of the sensor's output signal to the noise present in the output signal and can be expressed by the following:

$$SNR = \frac{\mu}{\sigma}$$

Where μ is the mean signal and σ is the standard deviation of the signal.

This assessment was performed on the product detailed in Table 4-1.

Table 4-1: HyperScan Products over Libya-4

Product	Site	Product Name (JL1GP)	Sensor Viewing Angle (°)
1	Libya-4	02_PMS1_20210502183238_200048728_103_0002_001_L3A	12.00

The approach developed for EDAP applies filtering to remove non-homogenous areas and so produces a more consistent result. The steps include:

1. Compute the local statistics of a small (3 x 3 pixels) sliding window applied to the imagery being assessed. Then, select only the "best" (in practice, this uses a Sobel filter and threshold of 1.0) small windows for the following steps.
2. Compute the statistical distribution (histogram), between the **minimum** and **maximum radiance**, of the selected "best" small windows (statistics of 3 x 3 pixel windows) – the signal is defined as the peak (i.e. mean radiance) of this statistical distribution, and the noise is defined as the standard deviation of this statistical distribution about the mean.

4.2.2.2 Results

The results include a plot for each band (only a single band is shown, which is band 5 as that is used as the red band when displaying RGB images); see Figure 4-2.

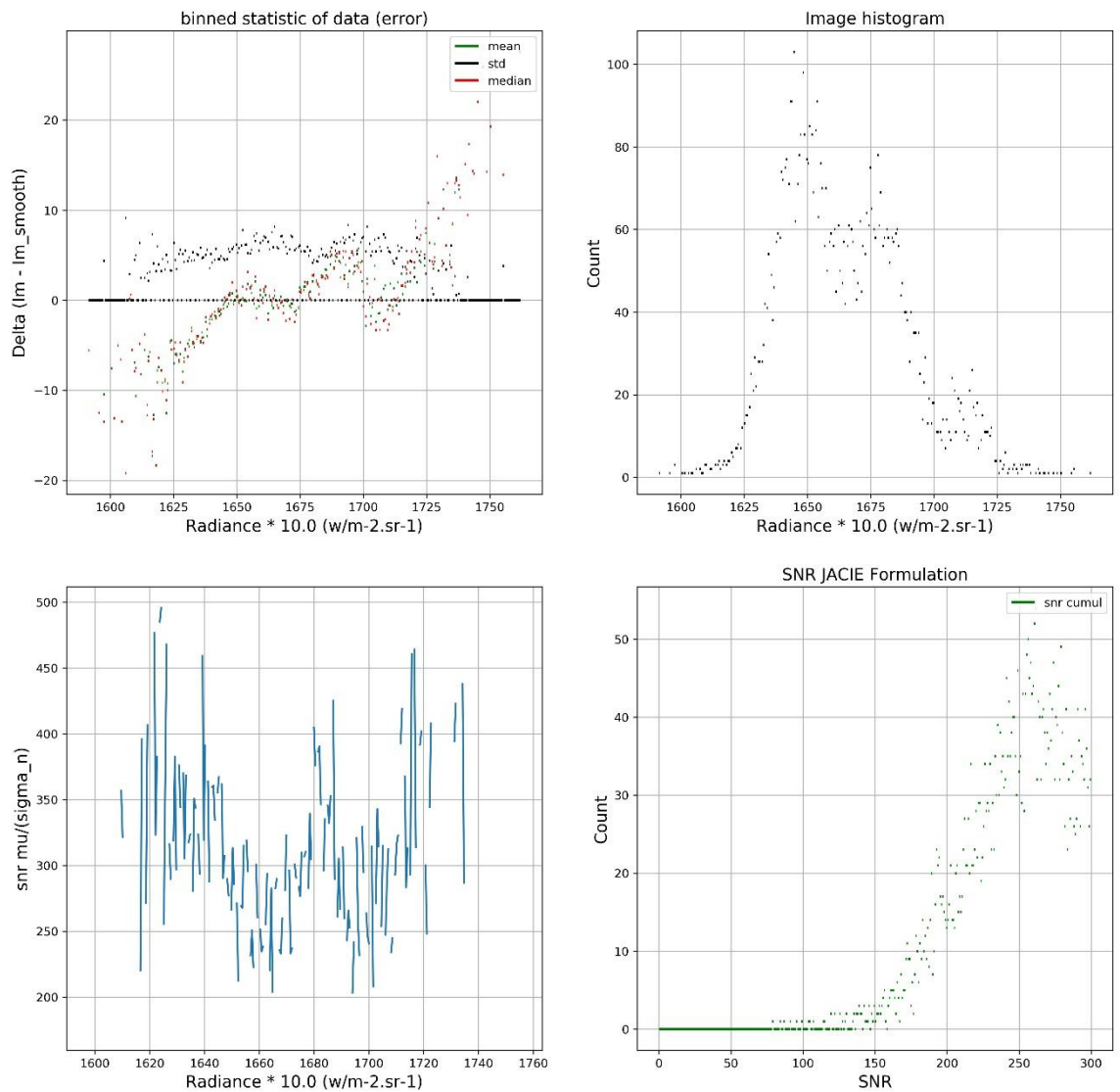
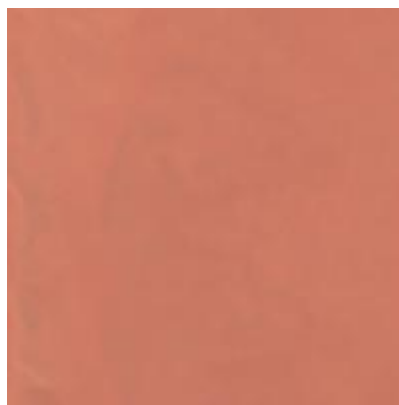


Figure 4-2: SNR plots for the 02 May 2021 band 5 (562.5 nm, green band) in terms of the binned statistics, image histogram and SNR using the simple formula plus cumulative SNR using the adapted formula.

Figure 4-3 then shows the spectral SNR for the image acquired over Libya-4.



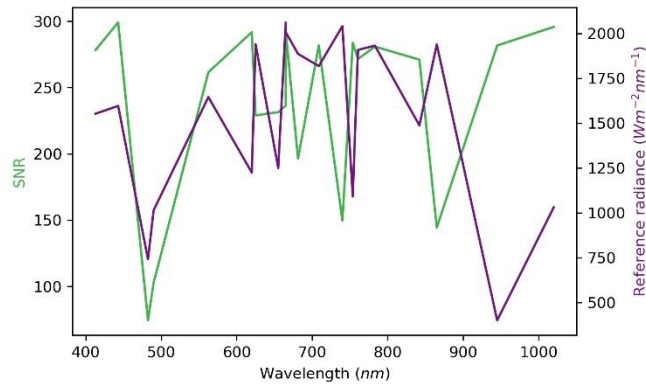


Figure 4-3: Subset of the HyperScan acquisition used (top) and SNR spectral plot (bottom) showing the estimated SNR and reference radiance for all the VNIR bands 02 May 2021 image.

A comparison of the calculated SNR values with the product metadata SNR values, provided in the quality metadata file for the first seven bands at a 5m spatial resolution and including the panchromatic band, is detailed in Table 4-2. The calculated values are significantly higher and band 3 is calculated as being low, which becomes more evident when all the bands are shown as in Figure 4-3.

Table 4-2: HyperScan SNR comparison for Libya-4

Band (central wavelength, nm)	Operator SNR	EDAP SNR
Panchromatic	41.302	228.977
1 (413)	34.753	278.365
2 (443)	35.478	299.185
3 (482.5)	36.376	74.250
4 (562.5)	35.890	261.618
5 (655)	36.972	231.442
6 (842)	37.598	271.107

4.2.3 Modulation Transfer Function

A sensor's spatial resolution has traditionally been a difficult concept to define. Still, it is linked to the Ground Sampling Distance (**GSD**) and Instantaneous Field of View (**IFOV**) of an imaging sensor system.

Note: As a measure of the geospatial quality of imagery, the MTF of the sensor is often used along with the SNR.

4.2.3.1 Method

Although the artificial MTF target located in Salon-de-Provence (France) was captured by the image acquired on the 07 April 2021, see Figure 4-4, this target is too small for the spatial resolution of this mission.



Figure 4-4: Salon-de-Provence MTF target as captured on the 07 April 2021 shown using the 5m resolution panchromatic band (left) and as shown using Google Earth (right) for the same geographical extent.

4.2.3.2 Results

Not assessed for this mission.

4.3 Geometric Calibration Quality

This section describes the assessment of geometric calibration quality, implemented by the processing chain, of sensor products in terms of **absolute geolocation accuracy**, **temporal geolocation accuracy** and **band co-registration accuracy**.

4.3.1 Absolute Geolocation Accuracy

The absolute geolocation (planimetric / horizontal) accuracy of the imagery is assessed through visual comparison with Sentinel-2 for the products detailed in Table 4-3.

Table 4-3: HyperScan Products over La Crau

Product	Site	Product Name (JL1GP)	Sensor Viewing Angle (°)
2	La Crau	02_PMS2_20210407194948_200046458_103_0002_001_L3A	23.20

The imagery included in this product has been used to determine the geolocation accuracy of *relatively low and homogenous topographies*. Note the topography of La Crau does not exceed 190 m above the ellipsoid. The HyperScan imagery have been corrected using a Digital Elevation Model (**DEM**), with the source being the Shuttle Radar Topography Mission (**SRTM**) at 90 m resolution (SRTM90). Since March 2021, the DEM used for the orthorectification of the Sentinel-2 L1C data is the Copernicus DEM GLO-90m [RD-6], prior to that it was the Planet-DEM-90 [RD-7] based on ASTER and SRTM.

4.3.1.1 Method

The visual comparison used Sentinel-2 Level 1 imagery acquired on the same, or nearby, dates as the HyperScan imagery, and so close in time. The Sentinel-2 data was read into SNAP and then exported as a GeoTIFF. Then, the combined Sentinel-2 / HyperScan products were visualised in QGIS.

4.3.1.2 Results

Figure 4-5 compares the same areas (at three zoom settings from the whole image down to a small region) for Sentinel-2 and HyperScan on 07 April 2021. The effects of the different spatial resolutions, 10 m versus 30 m, can be seen alongside a displacement.



Figure 4-5: Comparison of 07 April 2021 Sentinel-2 pseudo-true colour and HyperScan panchromatic imagery for La Crau at various zoom settings with RadCalNet location as a yellow point: top overlaid, showing full HyperScan extent and then bottom zooming in to show (left) HyperScan and (right) Sentinel-2 separately.

Figure 4-6 shows Sentinel-2 as the backdrop image with the overlaid GCP locations for the Sentinel-2 image (red) and VNIR HyperScan (blue). The average difference, for the x and y directions, compared to Sentinel-2 for the four locations was: -4.507 m and 5.045 m.

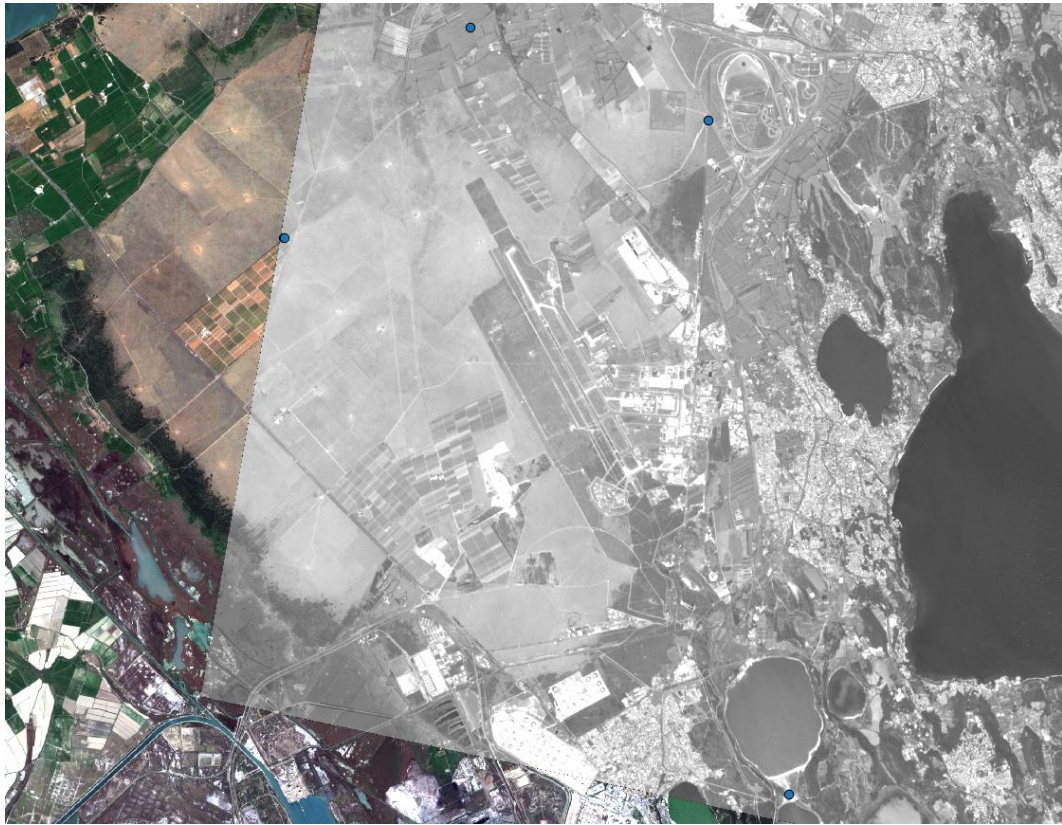


Figure 4-6: Comparison of Sentinel-2 07 April 2021 (image and red points) overlaid within GCPs for the same features digitised from VNIR HyperScan for 18 March 2020 (blue) – it is difficult to see the red points because, visually, they are under the blue points.

4.3.2 Temporal Geolocation Accuracy

The temporal planimetric geolocation accuracy (i.e. stability) of the imagery is determined by comparing imagery sensed at different points in time. Note: no minimum requirement has been specified for temporal planimetric geolocation accuracy.

This assessment was not performed for La Crau as there was only a single image acquired, but multiple images were acquired at other sites.

4.3.2.1 Method

This method requires several images over a single test site, which was available over Barrax where the images shown in Table 4-4 were acquired.

Table 4-4: HyperScan Products over Barrax and Rame

Product	Site	Product Name (JL1GP)	Sensor Viewing Angle (°)
3	Barrax	02_PMS2_20200518202517_200025742_102_0007_001_L3A	10.87
4	Barrax	01_PMS2_20210322202050_200044791_101_0005_001_L3A	13.71

5	Rame	02_PMS1_20210402204219_200045974_102_0001_001_L3A	12.59
6	Rame	01_PMS1_20210423205119_200047910_102_0001_001_L3A	11.24

The comparison follows the technique shown in Section 4.3.1, i.e., locating recognisable features in both the Sentinel-2 and HyperScan imagery and comparing the geolocation.

4.3.2.2 Results

Figure 4-7 shows Sentinel-2 as the backdrop image for Barrax, with the overlaid GCP locations for the Sentinel-2 image (red) and VNIR HyperScan for 18 May 2020 (blue) and 22 March 2021 (purple). The average differences, for the x and y directions, compared to Sentinel-2 for the four locations were:

- Product 1, 18 May 2020: -3.265 m and -28.686 m
- Product 2, 22 March 2021: 8.340 m and -1.056 m

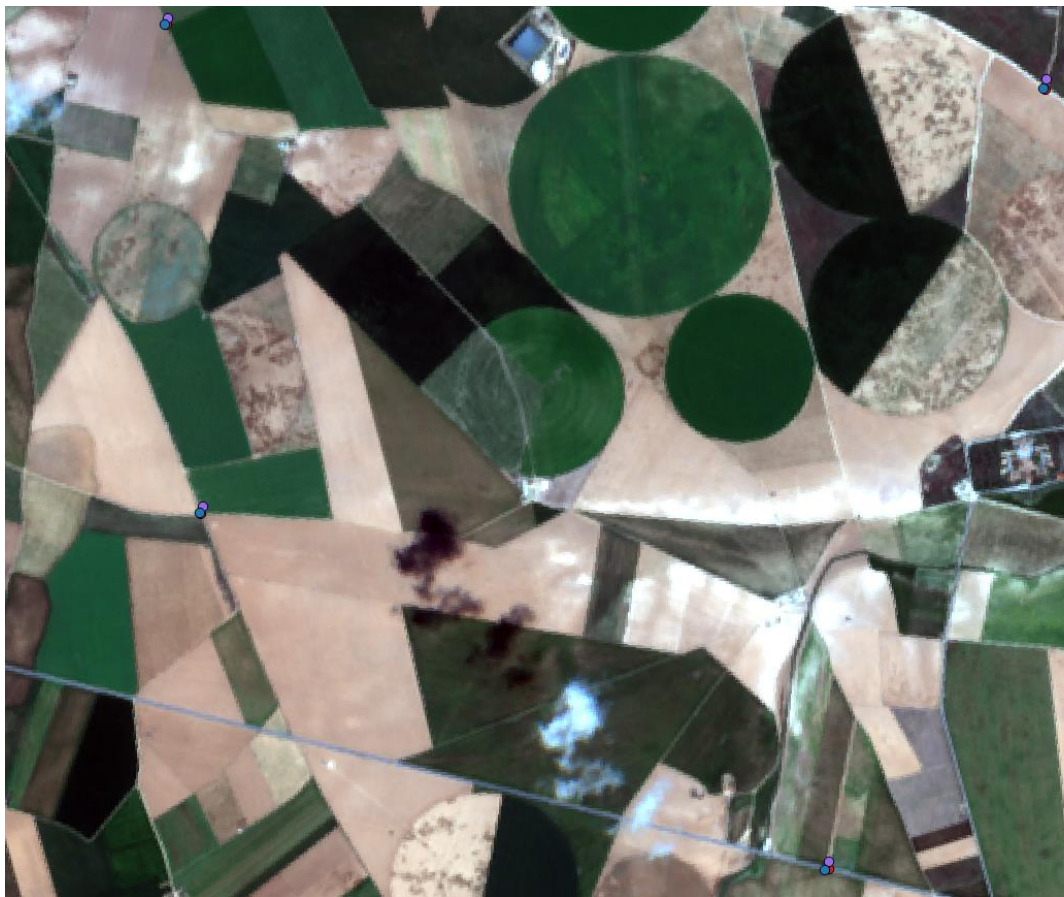


Figure 4-7: Comparison of Sentinel-2 18 May 2020 (image and red points) overlaid within GCPs for the same features digitised from VNIR HyperScan for 18 May 2020 (blue) and 22 March 2021 (purple) – it is difficult to see the red points because, visually, they are under the blue and purple points.

For Rame Head, as shown in Figure 4-8, the differences were:

- Product 3, 02 April 2021: -3.265 m and -28.686 m
- Product 4, 23 April 2021: 8.340 m and -1.056 m



Figure 4-8: Comparison of Sentinel-2 24 April 2021 (image and red points) overlaid within GCPs for the same features digitised from VNIR HyperScan for 02 April 2021 (blue) and 23 April 2021 (purple) – it is difficult to see the blue and purple points because, visually, they are under the red points.

4.3.3 Band Co-registration Accuracy

A visual analysis was performed for the band co-registration assessment.

4.3.3.1 Method

Each band is stored in a different GeoTIFF file, and the geometric information held within those files varies, so a single file containing all bands was created, and the coarser spatial resolution bands resampled to 5 m, using GDAL.

4.3.3.2 Results

The visual inspection of these images, see Figure 4-1, indicated there were no visible anomalies or artefacts. Taking the acquisition of La Crau and zooming in to an area with significant spatial variation shows that we are not seeing any apparent band-to-band pixel shift when bands with different spatial resolutions are shown together; see Figure 4-9.



Figure 4-9: Zoomed-in examples for La Crau acquired on the 22 March 2021 as pseudo-true colour data with bands (left) of the same 5m resolution using 655 [8], 562.5 [5] and 482.5 [3] nm and (right) of varying resolution using 665 [9, 5 m], 490 [4, 10 m] and 443 [3, 5 m] nm.

4.4 Radiometric Calibration Quality

This section describes the assessment of radiometric calibration quality of sensor products, in terms of **absolute** and **temporal radiometric calibration accuracy**.

4.4.1 Absolute Radiometric Calibration Accuracy

RadCalNet is an initiative of the Working Group on Calibration and Validation of the Committee on Earth Observation Satellites (**CEOS**). The RadCalNet service provides satellite operators with SI-traceable Top of Atmosphere (**TOA**) spectrally-resolved reflectances to aid in the post-launch radiometric calibration and validation of optical imaging sensor data [RD-8].

The free and open access service provides a continuously updated archive of TOA reflectances derived over a network of sites, with associated uncertainties, at a 10 nm spectral sampling interval, in the spectral range from 380 nm to 2500 nm and at 30-minute time intervals.

4.4.1.1 Method

4.4.1.1.1 Comparison to RadCalNet

The method used for this assessment consists of different processing stages, as shown in Figure 4-10; this approach is used across several mission assessments and further details are in the DOVE-R Technical Note [RD-9]. The approach was implemented in a series of Jupyter notebooks so that the analysis can easily be rerun.

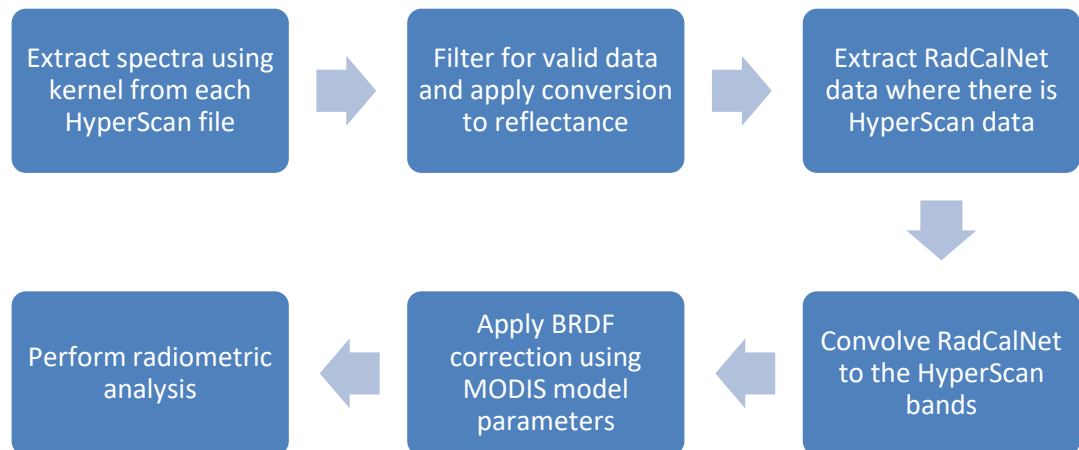


Figure 4-10: The workflow of the radiometric calibration assessment using RadCalNet data.

These different processing stages can be summarised as follows:

- Extract multispectral TOA measurements from the HyperScan products collected over the La Crau (France) RadCalNet station, and convert to reflectance using the supplied Solar Irradiance data with a correction for the Earth-Sun-Distance (related to the time of year) and viewing geometry.
- The measurement is spatially integrated over a 5 x 5 kernel, which is a window of size of 25 x 25 m, where there is valid data.
- Extract the RadCalNet TOA estimates where there is valid HyperScan data. As the RadCalNet measurements are provided every 30 minutes, it is not possible to get a RadCalNet matchup at the exact time of the HyperScan product acquisition, therefore linear temporal interpolation is performed to reduce the influence of this time-difference.
- Convolve the RadCalNet 10 nm TOA spectrum with the HyperScan spectral bands to get the reference measurements for each sensor spectral band – this involves linearly interpolating the RadCalNet data to the spectral resolution of the sensor’s relative spectral response and then multiplying by that response. As no spectral response data was provided for HyperScan, the RadCalNet data was linearly interpolated to 1 nm and then it was assumed each hyperspectral band had a square bandwidth of 5 nm with the given wavelengths being the central position.
- Application of the Bidirectional Reflectance Distribution Function (**BRDF**) correction to the HyperScan data using the model parameters in the MODIS albedo / BRDF product (MCD43A1) using the c-factor method as defined in [RD-10]:

$$NBAR = c_{\lambda} * \rho_{\lambda}(\theta_v = \theta_v^{HyperScan}, \theta_s = \theta_s^{HyperScan})$$

$$c_{\lambda} = \frac{\rho_{\lambda}^{MODIS}(\theta_v = 0, \theta_s = k)}{\rho_{\lambda}^{MODIS}(\theta_v = \theta_v^{HyperScan}, \theta_s = \theta_s^{HyperScan})}$$

where θ_v is the view zenith angle, θ_s is the solar zenith angle and k is the average solar zenith angle of the pair of forward and backward scattering observations. The MODIS reflectances are calculated from the model parameters in the MODIS product using the view and solar zenith and azimuth angles.

- Plot the convolved RadCalNet data against the HyperScan data, and also extract Sentinel-2 Level 1C data for comparison.
- Compute the calibration ratio between HyperScan mean TOA reflectance and RadCalNet TOA reflectance, then compute the percent difference as follows:

$$\%Difference = \frac{100 * (TOA_Measure - TOA_Reference)}{TOA_Reference}$$

Where *TOA_Measure* is the measurement processed from the HyperScan product, and *TOA_Reference* is the measurement processed from RadCalNet data.

As detailed in [RD-8], the TOA reflectance spectra over the La Crau RadCalNet site are representative of a disk of 30 m radius on latitude 43.55885° and longitude 4.864472°. This assessment uses the TOA observed radiance data, and the highest spatial resolution HyperScan pixels are 5 m in resolution, so a 5 x 5 kernel would equate to 25 m x 25 m. The coarser spatial resolution bands were interpolated to 5 m resolution as part of ingestion and so the kernel size is the same, the bit number of original pixels included will vary.

From Figure 4-11, it can be seen that the site is in the middle of an open area where there is limited spatial variation, although there are some spatial features further away than the HyperScan kernel being used – the site is flat but is intersected by field boundaries that include roads and buildings.



Figure 4-11: La Crau location on Sentinel-2 Level 1 image (18 March 2020), with the RadCalNet site location as a pin marker.

4.4.1.1.2 Comparison to CHRIS/Proba-1

A second method used for this assessment consists of comparing HyperScan to CHRIS/Proba-1, a mission that has been operating since October 2001. It has a stable calibration but is known to have some deviation from expected, with a significantly underestimation for the first band in Mode 1 (centred at 410 nm), and the slight overestimation in the NIR [RD-11]. The approach was implemented in a series of Jupyter notebooks so that the assessment can easily be rerun.

These different processing stages can be summarised as follows:

1. Extract multispectral TOA measurements from the HyperScan products collected over the Barrax and Rame Head and convert to reflectance using the supplied Solar Irradiance data with a correction for the Earth-Sun-Distance (related to the time of year) and viewing geometry.
2. The measurement is spatially integrated over a 5 x 5 kernel, which is a window of size of 25 x 25 m, where there is valid data.
3. Processing of the CHRIS/Proba-1 data and extraction for a 3 x 3 kernel, which is approximately 51 by 51 m.
4. Application of the BRDF correction to the HyperScan data; as described in the previous section.

- Plot the CHRIS/Proba-1 data against the HyperScan data, and also extract Sentinel-2 Level 1C data for comparison.



Figure 4-12: Barrax and Rame Head locations on contemporaneous Sentinel-2 Level 1 images (18 May 2020 and 24 April 2021), with the extracted point as a marker near the centre of the shown sub-area of the acquisition.

4.4.1.2 Results

4.4.1.2.1 Comparison to RadCalNet

The HyperScan solar and viewing geometry (mean values) and RadCalNet auxiliary data are shown in Table 4-5.

Table 4-5 HyperScan Sensor Observation Conditions (Solar and Viewing Geometries)

Product	Sensor Zenith Angle (°)	Sensor Azimuth Angle (°)	Solar Zenith Angle (°)	Solar Azimuth Angle (°)	Water Vapour (g/cm)	Aerosol Optical Depth (m-1)
1	23.20	119.62	36.72	183.82	0.08	0.056

The calibration results based on in-situ RadCalNet data are described by showing the steps involved, which have been implemented within a series of Jupyter notebooks. Figure 4-13 shows a plot of the TOA RadCalNet reflectance spectra for La Crau (LCFR) and the spectra convolved to the HyperScan bands for the 07 July 2021.

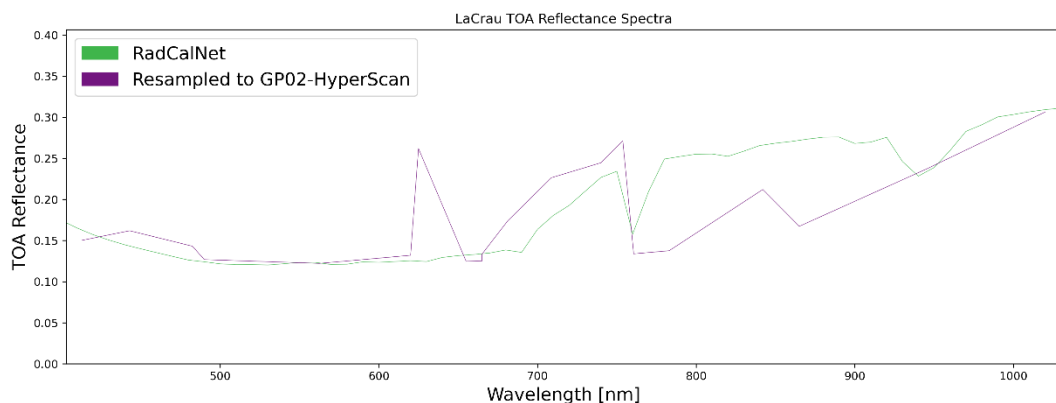


Figure 4-13: Convolution of the RadCalNet reflectance spectra into the HyperScan bands.

For each date in the RadCalNet series, an input HyperScan file is looked for and the data extracted with the two spectra being compared (Figure 4-14). The actual HyperScan data is plotted as the mean of the kernel with the vertical bars showing the standard deviation. The plot shows two versions of that data – before the Bidirectional Reflectance Distribution Function (BRDF) correction was applied and afterwards as the Nadir BRDF-Adjusted Reflectance (NBAR). The Sentinel-2 values, for the Level-1C images acquired on the same dates, have also been plotted as further reference values. The BRDF correction depends on the sun-satellite geometry, including the sensor zenith angle that was 23.2 degrees.

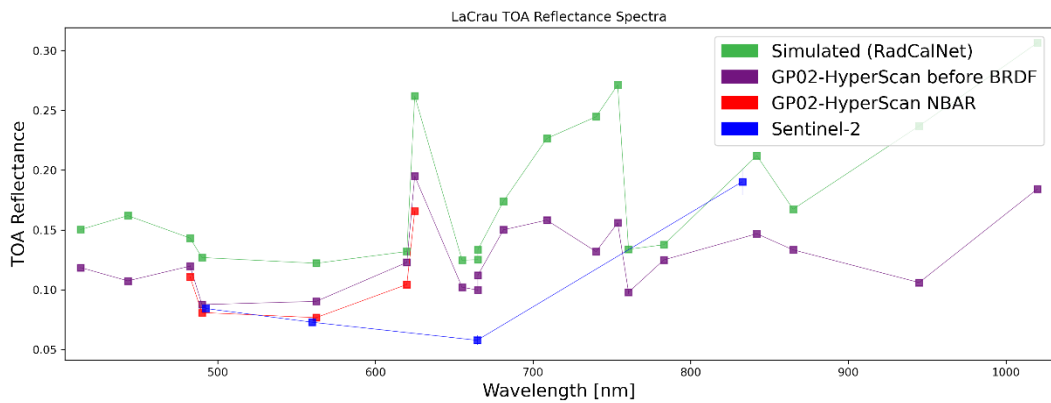


Figure 4-14: Comparison of HyperScan data (with and without BRDF correction, using supplied band convolved solar irradiance data) and RadCalNet convolved to the HyperScan bands.

Figure 4-15 shows a plot for all the HyperScan bands for the 07 July 2021 with valid data as a correlation plot. The line is the 1:1 relationship and each point is colour coded according to its wavelength, from blue through the black as we proceed through the visible and then Near-Infrared (NIR) bands.

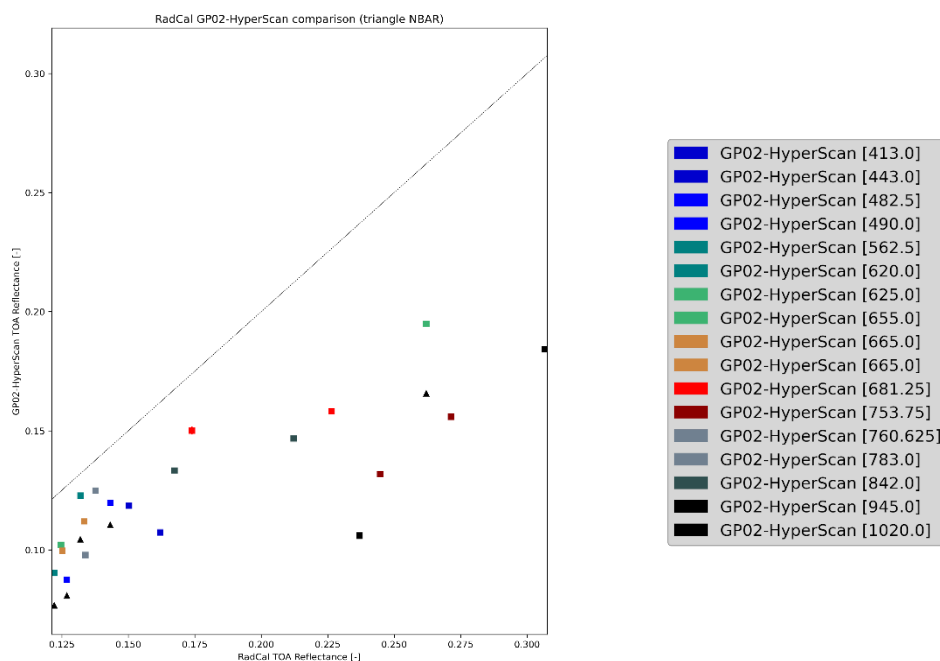


Figure 4-15: Comparison of HyperScan data with RadCalNet convolved to HyperScan for all dates, with a 1 to 1 line shown (square markers are without BRDF correction and triangles are with, NBAR).

Figure 4-16 shows the calculated percentage difference between the HyperScan 07 May 2020 and convolved RadCalNet data. As is also evident in Figure 4-15, all bands have lower values than the RadCalNet data.

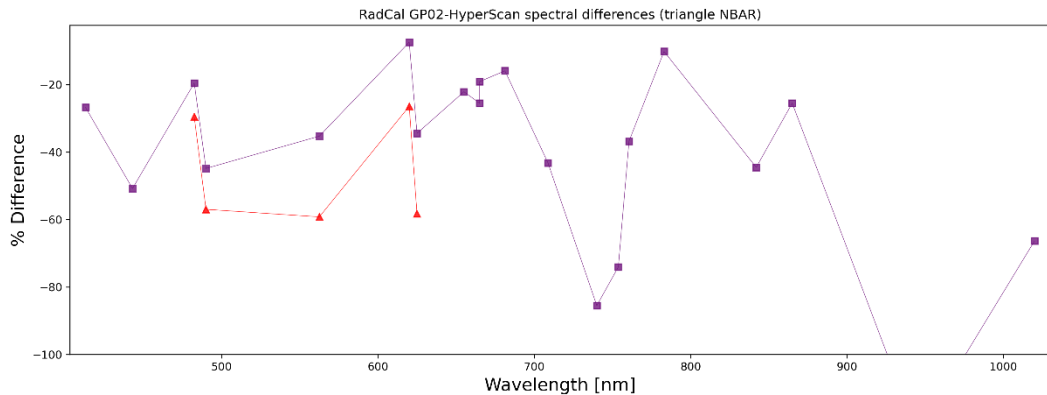


Figure 4-16: Spectral plot of the percentage differences between HyperScan and convolved RadCalNet data.

4.4.1.2.2 Comparison to CHRIS/Proba-1

The actual HyperScan data is plotted as the mean of the kernel with the vertical bars showing the standard deviation. The plot shows two versions of that data – before the Bidirectional Reflectance Distribution Function (**BRDF**) correction was applied and afterwards as the Nadir BRDF-Adjusted Reflectance (**NBAR**). The processed CHRIS/Proba-1 TOA and Sentinel-2 Level-1C images acquired on the same dates, have also been plotted as further reference values. The BRDF correction depends on the sun-satellite geometry, including the viewing zenith angle.

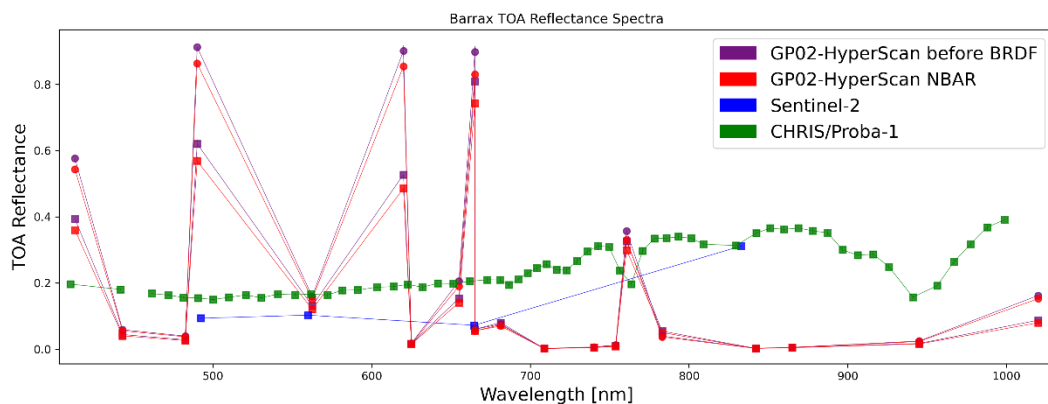


Figure 4-17: Comparison of HyperScan data (with and without BRDF correction) to CHRIS-Proba-1 for Barrax – soil site.

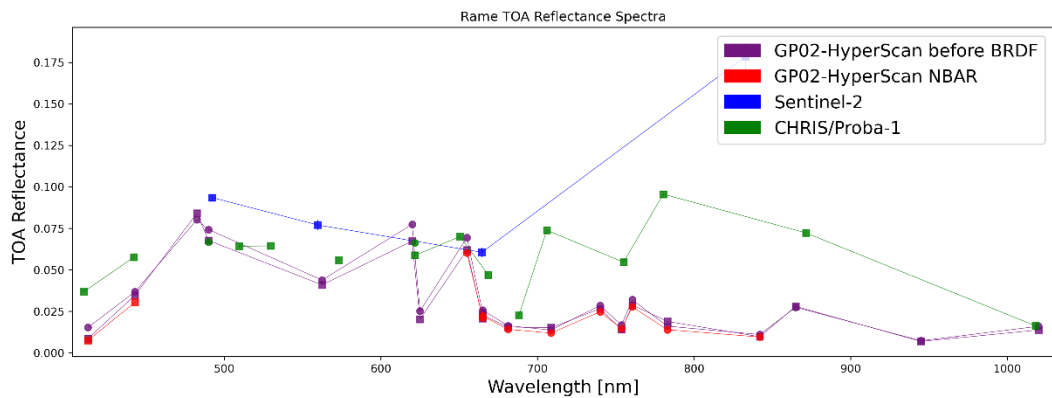


Figure 4-18: Comparison of HyperScan data (with and without BRDF correction) to CHRIS-Proba-1 for Rame Head – marine site.

4.4.2 Temporal Radiometric Accuracy

4.4.2.1 Method

As only one acquisition was available for La Crau, an assessment of the temporal radiometric accuracy was not possible using RadCalNet data. There were two acquisitions for Barrax and Rame Head, but the site at Rame Head is not stable temporally as it is over coastal waters. Therefore, only Barrax could be assessed.

4.4.2.2 Results

The results for the two acquisitions of Barrax (see Figure 4-17) show a consistency / stability for the radiometric values extracted although it is recognised this are limited datasets on which to perform this assessment.

5. CONCLUSIONS

This technical note details the high-level data quality assessments (including geometric calibration, radiometric calibration and image quality) that were performed on a sample of six, Level 3A (Standard Orthorectified) HyperScan products. Overall, the results of the aforementioned data quality assessments conclude that the performance of the sensor and the processing implemented are reasonable.

The results of the geometric calibration quality assessment indicate general agreement with the geolocation accuracy performance requirement, detailed in the HyperScan datasheet [RD-3] as < 20 m; there is no detail on how it is calculated so it is not clear if this is a CE90 value. For two acquisitions, the northing error was greater than 20 m, but the assessment was performed for a relatively small number of both GCPs and acquisitions. The metadata for the products, indicated the processing had not used GCPs and so these could be used to improve temporal accuracy.

The results of the radiometric calibration assessment found significant differences from what would have been expected using RadCalNet. The Jilin-1 instruments are vicariously calibrated over desert areas in Africa and China using MODIS surface reflectance data that is propagated to the top of atmosphere. Modified calibration coefficients are used where the relative difference between cross-calibration gain coefficients and ground calibration gain coefficients is greater than 10% [RD-5], but it is not clear from the metadata whether this has been applied. It may be that it has not been applied, or that it has but the approach/sites currently used does not fully capture the sources of error that we are capturing with the EDAP assessment.

APPENDIX A HYPERSCAN TEST DATASET

Table 5-1: HyperScan Products over La Crau, Libya-4, Barrax and Rame

Product	Site	Product Name	Sensor Viewing Angle (°)	Quality Assurance File
1	La Crau	JL1GP02_PMS2_20210407194948_200046458_103_0002_001_L3A	23.20	Yes
2	Libya-4	JL1GP02_PMS1_20210502183238_200048728_103_0002_001_L3A	12.00	Yes
3	Barrax	JL1GP02_PMS2_20200518202517_200025742_102_0007_001_L3A	10.87	No
4	Barrax	JL1GP01_PMS2_20210322202050_200044791_101_0005_001_L3A	13.71	No
5	Rame	JL1GP02_PMS1_20210402204219_200045974_102_0001_001_L3A	12.59	Yes
6	Rame	JL1GP01_PMS1_20210423205119_200047910_102_0001_001_L3A	11.24	Yes



[END OF DOCUMENT]